Matters arising

DHODH inhibitors sensitize to ferroptosis by FSP1 inhibition

https://doi.org/10.1038/s41586-023-06269-0

Received: 13 September 2022

Accepted: 30 May 2023

Published online: 5 July 2023

Check for updates

Eikan Mishima[1,2,5], Toshitaka Nakamura[1,5], Jiashuo Zheng[1,5], Weijia Zhang[1], André Santos Dias Mourão[3], Peter Sennhenn[4] & Marcus Conrad[1]✉

ARISING FROM C. Mao et al. *Nature* https://doi.org/10.1038/s41586-021-03539-7 (2021)

Ferroptosis, a form of non-apoptotic cell death that is hallmarked by lipid peroxidation of cellular membranes, has gained considerable attention as it is considered a potential therapeutic target for breaking cancer therapeutic resistance[1]. In their recent Article, Mao et al.[2] identified mitochondrially localized dihydroorotate dehydrogenase (DHODH) as an additional enzyme that mediates suppression of ferroptosis, implying that inhibition of DHODH may present a promising strategy to overcome ferroptosis resistance in cancer cells. Here we show that the contribution of DHODH in ferroptosis suppression appears to be small and context-dependent, because the ferroptosis-sensitizing effect of DHODH inhibitors is apparent only at high concentrations that also efficiently inhibit ferroptosis-suppressor protein 1 (FSP1), which has an important role in ferroptosis defence[3]. The observed effects on ferroptosis sensitization with this concentration of inhibitors cannot be attributed to DHODH inhibition per se. Thus, applying compounds that modulate ferroptosis at appropriate concentrations is mandatory to avoid off-target effects.

Canonically, DHODH catalyses the ubiquinone (CoQ_{10})-dependent oxidation of dihydroorotate to orotate. Orotate is an essential building block for the de novo pyrimidine biosynthesis that is required during cell proliferation, and therefore DHODH presents a promising target for tumour therapy[4] (Extended Data Fig. 1a). Mao et al.[2] concluded that in addition to the mitochondrial form of glutathione peroxidase 4 (GPX4), DHODH is able to suppress ferroptosis at the inner mitochondrial membranes by reducing CoQ_{10} to ubiquinol. Ubiquinol in turn facilitates the scavenging of phospholipid radicals, which implies that DHODH may constitute a druggable target for ferroptosis sensitization[2]. Substantiating their conclusions, the authors showed that cancer cell lines with genetic deletion of *DHODH* were more sensitive to ferroptosis-inducing agents, including the GPX4 inhibitor (1*S*,3*R*)-RSL3 (RSL3). Moreover, they showed that brequinar, a potent and selective inhibitor of DHODH, also sensitized cancer cells towards ferroptosis. Although a comprehensive mechanistic framework explaining the molecular events that ultimately determine the cells' sensitivity to ferroptosis is an important goal for the ferroptosis field, the study by Mao et al.[2] contains several weaknesses and misinterpretations, strongly arguing against the conclusion that inhibition of DHODH is a promising target to overcome ferroptosis resistance in cancer cells.

First, the authors used extremely high concentrations of brequinar (500 μM), far exceeding the reported half-maximal inhibitory concentration (IC_{50}) of 7 nM, to inhibit DHODH[4,5]. Although we could indeed observe a synergistic effect of brequinar and ferroptosis inducers, including RSL3, in various cancer cells (Fig. 1a and Extended Data Fig. 1b–d), the sensitizing effect of brequinar was only evident at a concentration (IC_{50} = 61 μM; Fig. 1a) much higher than that required for DHODH inhibition (Fig. 1b and Extended Data Fig. 1e). DHODH is a CoQ_{10}-reducing flavoprotein similar to FSP1, which suppresses ferroptosis by reducing extramitochondrial CoQ_{10} and vitamin K[3,6], thereby preventing lipid peroxidation in a wide array of cancer cell lines independently of the cysteine–glutathione–GPX4 axis. Thus, we tested whether the ferroptosis-sensitizing effect of brequinar was actually mediated by inhibition of FSP1. Indeed, cell-free assays using recombinant FSP1 revealed that high concentrations of brequinar inhibited FSP1 activity (IC_{50} = 24 and 14 μM for human and mouse FSP1, respectively), similar to the human FSP1-specific inhibitor iFSP1[3] (Fig. 1c and Extended Data Fig. 2a–c). In line with this result, the high concentration of brequinar also induced ferroptosis in mouse fibroblast Pfa1 cells with genetic deletion of *Gpx4* and stably overexpressing human FSP1, whose survival depends solely on FSP1 activity[3] (Fig. 1d). Notably, the ferroptosis-sensitizing effect of brequinar was retained regardless of the genetic ablation of *DHODH* (Fig. 1e and Extended Data Fig. 2d), whereas it was lost in *FSP1*-knockout cells (Fig. 1f). Of note, other DHODH inhibitors (for example, vidofludimus) also showed FSP1 inhibitory effects and sensitized cells to ferroptosis (Extended Data Fig. 2e–h), whereas BAY-2402234, a DHODH inhibitor seemingly lacking FSP1 inhibitory activity, did not sensitize cells towards ferroptosis (Extended Data Fig. 2h). Predictive structural analysis suggested that brequinar fitted well in the putative CoQ_{10}-binding pocket of FSP1 (Fig. 1g and Extended Data Fig. 2i). Together, these results demonstrate that the ferroptosis-sensitizing effect of brequinar (and several other DHODH inhibitors) is mediated via inhibition of FSP1 and not via DHODH.

Second, Mao et al.[2] report that genetic deletion of *DHODH* potently sensitized human cancer cells, including HT-1080 cells, to ferroptosis induced by RSL3[2]. Nonetheless, in our hands this sensitizing effect by deletion of DHODH was minor and far smaller than the effect of *FSP1* deletion (Fig. 1h and Extended Data Fig. 3a). This tendency was even more apparent in other cancer cell lines (Fig. 1h). In addition, unlike FSP1, overexpression of DHODH invariably did not protect Pfa1 cells from ferroptosis induced by genetic deletion of *Gpx4* or by inhibition of GPX4 with RSL3 (Fig. 1i and Extended Data Fig. 3b,c). By stark contrast, overexpression of FSP1 alone was sufficient to prevent ferroptosis even in the absence of GPX4 and DHODH expression (Extended Data Fig. 3d,e). As such, the contribution of DHODH to ferroptosis resistance seems to be rather subtle.

Third, the concentration of RSL3 used by Mao et al.[2] to induce ferroptosis in HT-1080 cells was very high. HT-1080 is among the most

[1]Institute of Metabolism and Cell Death, Helmholtz Zentrum München, Neuherberg, Germany. [2]Division of Nephrology, Rheumatology and Endocrinology, Tohoku University Graduate School of Medicine, Sendai, Japan. [3]Institute of Structural Biology, Helmholtz Zentrum München, Neuherberg, Germany. [4]transMedChem, Munich, Germany. [5]These authors contributed equally: Eikan Mishima, Toshitaka Nakamura, Jiashuo Zheng. ✉e-mail: marcus.conrad@helmholtz-munich.de

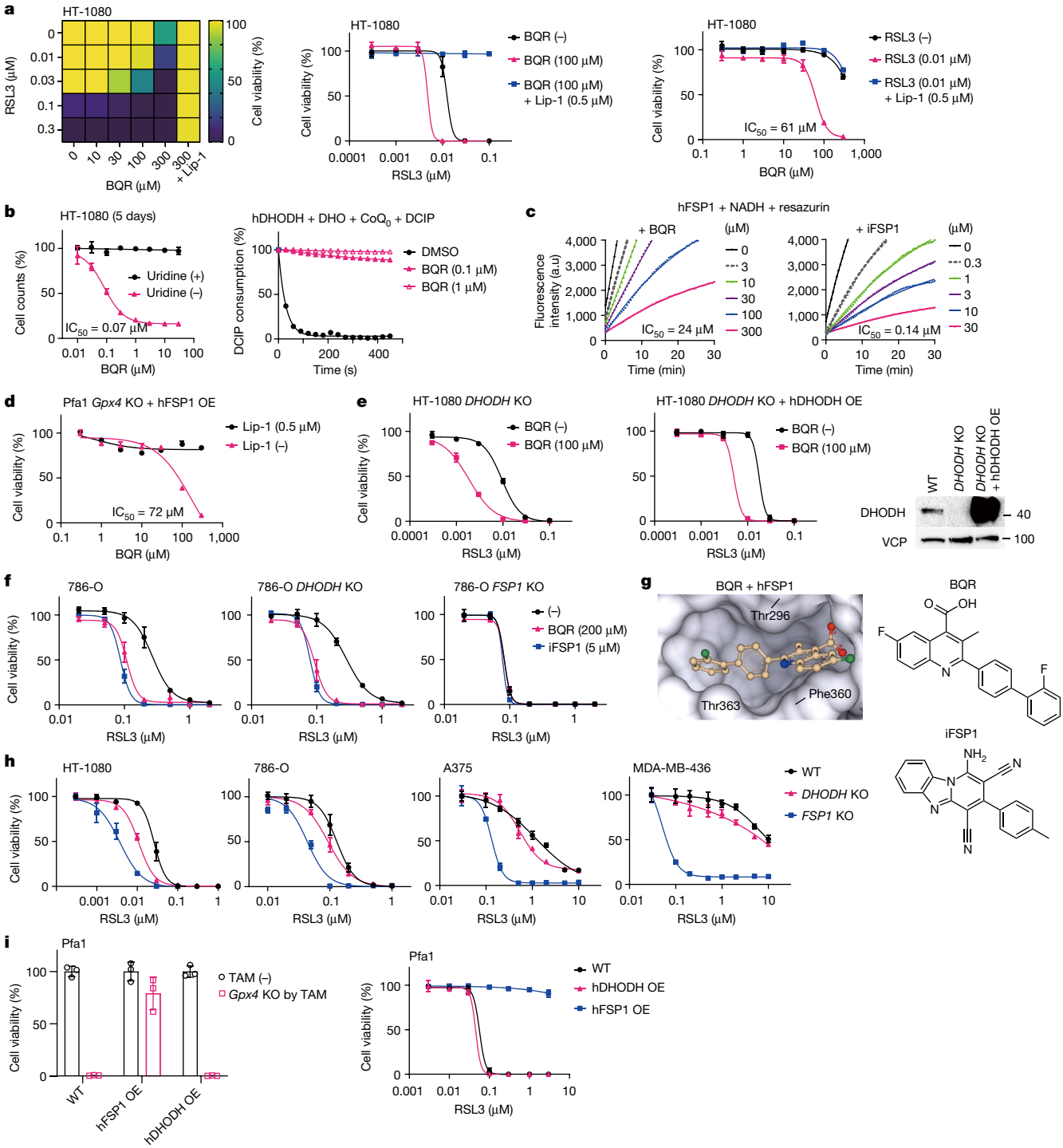

Fig. 1 | Brequinar sensitizes cancer cells to ferroptosis via FSP1 inhibition. **a**, Left, heat map of viability of HT-1080 cells showing the synergistic lethal effects of brequinar (BQR) and RSL3. The well-established ferroptosis inhibitor liproxstatin-1 (Lip-1, 0.5 μM) was used as a positive control to prevent ferroptosis. Viability was measured after treatment with RSL3 for 24 h. Middle, viability of HT-1080 cells treated with varying concentrations of RSL3 and a fixed concentration of BQR (100 μM) for 24 h. Right, viability of HT-1080 cells treated with increasing concentrations of BQR and a sub-lethal dose of RSL3 (0.01 μM) for 24 h. **b**, Left, relative cell counts of BQR-treated HT-1080 cells incubated with or without uridine (100 μM) for 5 days. Right, in vitro assays showing the inhibitory effect of BQR (0.1 and 1 μM) on DHODH enzyme activity. Recombinant human DHODH (hDHODH, 25 nM), dihydroorotate (DHO), coenzyme Q_0 (CoQ_0) and 2,6-dichloroindophenol (DCIP) were used. **c**, In vitro assays showing the inhibitory effect of BQR and iFSP1 towards FSP1 enzyme activity. Recombinant human FSP1 (hFSP1, 50 nM) was used. a.u., arbitrary units. **d**, The effect of BQR on the viability of Pfa1 mouse embryonic fibroblasts with *Gpx4* knockout (KO) and stable overexpression (OE) of human FSP1. **e**, The synergistic effect of BQR (100 μM) and RSL3 (24 h) on the viability of *DHODH*-knockout HT-1080 cells with or without overexpression of human DHODH. WT, wild type. **f**, The effect of BQR (200 μM) and iFSP1 (5 μM) on the viability of wild-type and *DHODH*- or *FSP1*-knockout 786-O cells treated with RSL3 for 24 h. **g**, Chemical structures of BQR and iFSP1 and the predicted binding site of BQR in the hFSP1 enzyme. **h**, The effects of genetic deletion of *DHODH* or *FSP1* on the viability of HT-1080, 786-O, A375 and MDA-MB-436 cancer cell lines treated with RSL3 for 24 h. **i**, Viability of wild-type or 4-hydroxytamoxifen (TAM)-induced *Gpx4*-knockout Pfa1 cells stably overexpressing haemagglutinin-tagged hFSP1 or hDHODH. Left, viability was measured three days after TAM treatment. Right, viability was measured after treatment with RSL3 for 24 h. Data are mean ± s.d. of $n = 3$ independent experiments (**a**,**b** (left), **d**–**f**,**h**,**i**). Data are representative of two (**b**, right) or three (**c**) independent experiments.

ferroptosis-sensitive human cancer cell lines and is thus widely used in ferroptosis research. On the basis of our own results as well as those from other groups, 300 nM of RSL3 is generally sufficient to induce ferroptosis in these cells (although fetal bovine serum contained in the culture medium may have an effect on ferroptosis sensitivity owing to variable concentrations of selenium, vitamin E and/or other micronutrients). The authors used more than 10 μM RSL3 to induce ferroptosis in HT-1080 cells[2]. These high concentrations were apparently necessary because the authors worked with very high cell densities, seeding 20,000 cells per well in a 96-well plate. It should be highlighted that high cell densities can indeed desensitize cells to ferroptosis and even protect *Gpx4*-knockout cells from dying[7,8] (Extended Data Fig. 3f). Besides GPX4, RSL3 targets most of the 25 human selenoproteins owing to the strong preference of the chloroacetamide group of RSL3 towards selenocysteine[9] (which probably becomes even more relevant at the higher concentrations as used here (over 10 μM)), therefore we assumed that the confluent cell culture conditions seem to be suboptimal when examining the ferroptosis sensitivity of the cells against RSL3.

Finally, the role of the mitochondrial form of GPX4 in ferroptosis prevention claimed by Mao et al.[2] is unclear. Here, it is important to mention that GPX4 is expressed in three distinct isoforms (Extended Data Fig. 4a). Transcription of the short form of GPX4 (the cytosolic form) is driven by its promoter 5′ of exon 1, whereas the mitochondrial matrix form is driven by a distal promoter that allows translation of a cognate mitochondrial targeting signal at its N terminus. Transcription of nuclear GPX4 is mediated by its own promoter in an alternative exon[10]. The short form of GPX4 is abundantly expressed in all tissues and is enriched in the cytoplasm and the extra-matrix space of mitochondria of somatic cells, whereas the mitochondrial matrix and nuclear forms are abundantly expressed in the mitochondrial matrix and nucleus of testicular cells, respectively[11,12] (Extended Data Fig. 4b). Earlier studies using isoform-specific knockout and transgenic mice as well as cells showed that the mitochondrial matrix and nuclear form are both important for spermatogenesis, but are otherwise dispensable for cytoprotection[12–14], although the influence of the knockout of the mitochondrial matrix-targeted variant of GPX4 in cancer cells has not been determined. Of note, although Mao et al. first reported that mitochondrial GPX4 has a role in ferroptosis prevention[2], a subsequent report by the same group reconciled their findings by showing that ferroptosis induced by *GPX4* deletion can only be prevented by overexpression of cytosolic GPX4 (that is, the short form) but not the mitochondrial matrix form[15], which is in agreement with our data (Extended Data Fig. 4c). In addition, the mitochondrial matrix form of GPX4 was expressed at a much lower level than the short form across a range of cancer cell lines, as determined by quantitative PCR with reverse transcription (RT–qPCR), the only way to unequivocally discriminate between the two forms (Extended Data Fig. 4d), similar to results from an earlier study performed on mouse tissues[11].

In summary, DHODH inhibitors, including high concentrations of brequinar, sensitize cancer cells to ferroptosis via inhibition of FSP1 and not DHODH. Appropriate concentrations of ferroptosis-inducing and -sensitizing compounds are needed to avoid off-target effects. Although a number of DHODH inhibitors have been developed and are in clinical development against solid and haematological malignancies[4], our study shows that the concentration and target engagement of DHODH inhibitors need to be carefully evaluated. Furthermore, we reiterate the importance of cell density in the study of ferroptosis and the seemingly irrelevant role of mitochondrial matrix GPX4 in ferroptosis prevention. The contribution of DHODH in ferroptosis, however, seems to be minor and context-specific.

Methods

Chemicals

Brequinar (SML0113), uridine (U3750), resazurin sodium salt (R7017), NADH (N8129), coenzyme Q_0 (D9150), 2,6-dichloroindophenol (DCIP, D1878), L-dihydroorotic acid (D7128), L-buthionine sulfoximine (BSO; B2515), menadione (M5625) and ferrostatin-1 (Fer-1, SML0583) were purchased from Sigma Aldrich. (1*S*,3*R*)-RSL3 (19288), ML210 (23282), vidofludimus (18377), BAY-2402234 (33259), and ASLAN003 (33516) were purchased from Cayman. The following chemicals were obtained as indicated: erastin (329600, Merck Millipore), iFSP1 (8009-2626, ChemDiv), liproxstatin-1 (Lip-1, S7699, Selleckchem), PCT299 (HY-124593, MedChemExpress).

Cell lines

TAM-inducible *Gpx4*$^{-/-}$ murine immortalized fibroblasts (Pfa1) were reported previously[7]. HT-1080 (CCL-121), 786-O (CRL-1932), A375 (CRL-1619), MDA-MB-436 (HTB-130), A549 (CCL-185), H460 (HTB-177), SW620 (CCL-227) and HEK293T (CRL-3216) cells were obtained from ATCC. LOX-IMVI was obtained from NCI/NIH. Cell lines, except for MDA-MB-436 and H460, were maintained in DMEM high glucose (4.5 g l^{-1} glucose, 21969-035, Gibco) supplemented with 10% fetal bovine serum (FBS), 2 mM L-glutamine, and 1% penicillin/streptomycin at 37 °C with 5% CO_2. MDA-MB-436 and H460 cells were maintained in RPMI 1640 medium (61870-010, GlutaMAX supplemented, Gibco) supplemented with 10% FBS and 1% penicillin/streptomycin. *DHODH*-knockout cells and *Dhodh*-knockout Pfa1 cells were maintained in a medium containing uridine (100 and 50 μM, respectively). *GPX4*-knockout cells were maintained in a medium containing Lip-1 (1 μM) or Fer-1 (5 μM). All cells were regularly tested for mycoplasma contamination.

Cell viability assays

Cells were seeded on 96-well plates at the following cell number per well and allowed to adhere overnight. For RSL3 treatment, 3,000 cells (HT-1080, 786-O and A375), 5,000 cells (MDA-MB-436) and 1,500 cells (Pfa1) were seeded. For the viability assay shown in a heat map, cells were seeded at 2,500 cells (HT-1080, 786-O, A375 and A549) and 5,000 cells (MDA-MB-436) for RSL3, ML210 and erastin treatment; and 1,000 cells of HT-1080 per well for BSO treatment. On the next day, cells were treated with the ferroptosis inducers. In the co-treatment experiments, brequinar, iFSP1 or Lip-1 were added alongside the ferroptosis inducers. When brequinar was used in the assay, uridine (100 μM) was supplemented in the media to avoid the effect of the depletion of intracellular pyrimidines as well as to maintain *DHODH*-knockout cells. Cell viability was assessed 24 h (RSL3 and ML210), 48 h (erastin) and 72 h (BSO) after the treatment using AquaBluer (MultiTarget Pharmaceuticals) or 0.004 % Resazurin sodium salt (Sigma Aldrich) diluted in the culture medium unless stated otherwise. The cell viability was expressed as relative values compared to the control sample, which was defined as 100%. To induce the knockout of *Gpx4* in Pfa1 cells, the cells were seeded on 96-well plates (500 cells/well) and treated with 1 μM TAM. Cell viability of TAM-treated Pfa1 cells was assessed 72 h after the treatment. To evaluate the effect of the confluency of cells towards ferroptosis sensitivity, HT-1080 cells were seeded on 96-well plates at 3,000, 8,000 and 20,000 cells per well, and then treated with RSL3 on the following day.

Cell proliferation assays

HT-1080 and Pfa1 cells were seeded on 96-well plates at 200 cells per well and incubated with or without uridine (100 and 50 μM, respectively) for 5 days. After the incubation, relative cell counts were evaluated using AquaBluer.

Preparation of lentiviral particles

Lentiviral packaging system consisting of a transfer plasmid, psPAX2 (12260, Addgene), with pMD2.G (for human cells, 12259, Addgene) or pHCMV-EcoEnv (for mouse cells, 15802, Addgene) was co-lipofected into HEK293T cells using PEI-MAX (Polysciences). Cell culture supernatants containing viral particles were collected 48 h after the transfection and used to transduce the cell line of interest after filtration using a 0.45 μm low protein binding syringe filter.

CRISPR–Cas9-mediated gene knockout

Sequences of single guide RNA (sgRNA), vectors for expression of Cas9 and sgRNA, and Cas9 expression system are listed in Supplementary Table 1. For transient expression of the CRISPR–Cas9 system, cells were transiently co-transfected with the sgRNA-cloned Cas9 expression plasmids (listed in Supplementary Table 1) using the X-tremeGENE HP agent (Roche). One day after transfection, cells were selected by treatment with puromycin (1 μg ml^{-1}), blasticidin (10 μg ml^{-1}) and/or geneticin (1 mg ml^{-1}). After selection, single-cell clones were picked and knockout clones were identified by immunoblotting. For stable expression of the CRISPR–Cas9 system, cells were infected with lentiviral particles containing the sgRNA-cloned lentiCRISPR v2-neo plasmid (98292, Addgene) with protamine sulfate (8 μg ml^{-1}). One day after transfection, cells were treated with geneticin (1 mg ml^{-1}). After the selection, the loss of expression of the targeted protein was confirmed by immunoblotting of batch cultures. For doxycycline-inducible Cas9 expression system, doxycycline-inducible Cas9 expressing cells were generated by transducing lentiviral particles containing pCW-Cas9-Blast (83481, Addgene)[6]. pCW-Cas9-Blast expressing cells were infected with lentiviral particles containing the sgRNA-cloned LentiGuide-Neo (139449, Addgene) or pKLV-U6gRNA(*Bbs*I)-PGKpuro2aBFP vector (50946, Addgene). One day after transfection, cells were treated with geneticin (1 mg ml^{-1}) or puromycin (1 μg ml^{-1}), and then incubated with doxycycline (10 μg ml^{-1}) for 5 days to express Cas9. After the selection and the Cas9 induction, single-cell clones were picked and knockout clones were identified by immunoblotting.

Overexpression of DHODH, FSP1 and GPX4 isoforms

Codon-optimized human *DHODH* gene with a C-terminal HA tag was synthesized (Twist Bioscience) and cloned in the expression vector pLV-EF1a-IRES-Neo (85139, Addgene). Human *FSP1*-coding original sequence (NM_001198696.2) with a C-terminal HA tag was cloned in the expression vector p442-Blast. Coding sequences of the short form (NM_001367832.1) and mitochondrial matrix form (NM_002085.5) of human *GPX4* were amplified by PCR using cDNA produced from A375 cells, and they were cloned into the expression vector p442-Blast. Cells were infected with lentiviral particles containing the transfer plasmids. One day after infection, cells were selected with geneticin (1 mg ml^{-1}) or blasticidin (10 μg ml^{-1}). Reconstitution of DHODH, FSP1 and GPX4 isoforms expression was verified by immunoblotting. *GPX4*-knockout HT-1080 cells overexpressing each form of GXP4 were maintained with Fer-1 (5 μM) after the selection.

Western blotting

Cells were lysed in LCW lysis buffer pH 7.5 (0.5% Triton X-100, 0.5% sodium deoxycholate salt, 150 mM NaCl, 20 mM Tris-HCl, 10 mM EDTA, 30 mM Na-pyrophosphate tetrabasic decahydrate) containing protease and phosphatase inhibitor mixture (cOmplete and phoSTOP, Roche), and centrifuged at 15,000*g*, 4 °C for 20 min. The supernatant was collected and used as the protein sample. Western blotting was performed by standard immunoblotting procedure with 12% SDS–PAGE gel, PVDF membrane, and primary antibodies against human FSP1 (1:1,000, sc-377120, Santa Cruz), DHODH (1:1,000, sc-166348, Santa Cruz), GPX4 (1:1,000, ab125066, Abcam), HA (1:1,000, clone 3F10, rat IgG1, developed in-house), and valosin containing protein (VCP) for loading control (1:10,000, ab109240, Abcam). Images were analysed with Image Lab 6.0 software (Bio-Rad).

Expression and purification of recombinant FSP1 and DHODH

Recombinant human and mouse FSP1 protein containing an N-terminal 6-histidine tag were produced in *Escherichia coli*, and purified by affinity chromatography with a Ni-NTA system as described previously[3]. The codon-optimized DNA sequence corresponding to the mitochondrial intermembrane region of human DHODH 29–395 was synthesized as a gBlocks gene fragment (Integrated DNA Technologies) and cloned into a petM11 vector that contains an N-terminal 6-histidine tag. Expression and purification were done as previously reported[16]. In short, *E. coli* BL21 cells were transformed with the prepared DHODH vector and grown in TB at 37 °C. When the cells reached OD 2.0, 0.5 mM IPTG was added and expression was performed at 20 °C overnight. Cells were collected, dissolved in the lysis buffer (PBS supplemented with 10 mM imidazole) and lysed using a sonicator. After centrifugation, the supernatant fraction was applied to a prepacked nickel column and washed extensively with the lysis buffer. The protein was eluted with PBS supplemented with 350 mM imidazole followed by concentration and final purification step over a size exclusion chromatography column pre-equilibrated with PBS. Protein was aliquoted, frozen in liquid nitrogen and stored at −80 °C until further usage.

FSP1 enzyme inhibitor assay

Enzyme reactions in PBS pH 7.4 containing 50 nM hFSP1 or mFSP1 enzyme, 200 μM NADH (freshly prepared in water) and the inhibitors were prepared[6]. After the addition of 100 μM resazurin sodium salt, fluorescent intensity (excitation 540, emission 590 nm) was measured every 30 s on a 96-well plate using a SpectraMax M5 Microplate Reader and SoftMAX pro 7 (Molecular devices).

Determination of FSP1 activity by measuring NADH consumption

Enzyme reactions in PBS pH 7.4 containing 25 nM hFSP1 and 50 μM of menadione with or without 300 μM of brequinar were prepared[6]. After the addition of 200 μM NADH, the absorbance at 340 nm was measured every 30 s on a 96-well plate. Reactions without NADH or without enzyme were used to normalize the results.

DHODH enzyme inhibitor assay

DHODH activity was measured as reported previously[17]. The reaction was performed at pH 8.0 at 32 °C in a buffer containing 50 mM Tris, 0.1% Triton X-100, 150 mM NaCl, 25 nM recombinant human DHODH protein, 500 μM L-dihydroorotic acid, 100 μM coenzyme Q_0 and 120 μM DCIP with the inhibitors. DHODH activity was measured kinetically as a function of decreased DCIP absorbance at 600 nm.

In silico modelling

The predicted human FSP1 structure was obtained from the AlphaFold2 database (https://alphafold.ebi.ac.uk)[18]. To yield the superposed structure of FSP1 with its cofactor flavin adenine dinucleotide (FAD), the structure of the yeast orthologue NDH-2 (Ndi1)[19] (PDB: 4G73) was aligned to FSP1 using Pymol v2.5.2 (Schrödinger), and the position of FAD was extracted and embedded into FSP1 structure as a template for modelling. The modelling software SeeSAR v12.1 (BioSoveIT) was used to dock the selected molecules into the hFSP1 protein. The binding site was detected and defined employing the integrated DoGSiteScorer module embedded in SeeSAR. Molecules were uploaded as SD files without any further preparation. For docking, the number of poses for each molecule was set to 500, and clash tolerance was set to high to allow a comparably tolerant generation of poses. The subsequent HYDE scoring function within SeeSAR was used to post-optimize the docking poses and to assess the estimated affinity. After visual inspection, the most viable poses were selected and filtered for favourable torsion quality and docking poses with unfavourable intra- and intermolecular clashes were removed.

RT–qPCR

Total RNA was extracted from the cells using RNeasy Mini kit (Qiagen) with genomic DNA removal by RNase-Free DNase set (Qiagen) and was reverse-transcribed using the QuantiTect Reverse Transcription Kit (Qiagen). Human testis mRNA was purchased from Takara-bio (636533)

and was reverse-transcribed. RT–qPCR was performed using PowerUp SYBR Green Master Mix (Thermo Fisher Scientific) with qTOWER3 G (Analytikjena). All samples were run with triplicates under the following condition:1, 50 °C for 2 min; 2, 95 °C for 2 min; 3, 95 °C for 15 s; 4, 59.5 °C for 15 s; 5, 72 °C for 1 min; 6, 95 °C 1 s and cycle from 3 to 5 was repeated for 40 times. Sequences of the primers were the following: 5′-TGCTCTGTGGGGCTCTG and 5′-ATGTCCTTGGCGGAAAACTC for detecting the short and mitochondrial matrix forms of *GPX4*; and 5′-ATTGGTCGGCTGGACGAG and 5′-ATGTCCTTGGCGGAAAACTC for specific detection of the mitochondrial matrix form. The expression ratio of (the mitochondrial matrix form)/(the short and mitochondrial matrix forms) of *GPX4* was calculated using the ΔC_t method.

Quantification and statistical analysis

Statistical information for individual experiments can be found in the corresponding figure legends. Values are presented as mean ± s.d. Statistical comparisons between groups were analysed by a two-tailed Student's *t*-test or one-way ANOVA with Dunnett's post hoc test. Statistical analyses were conducted using GraphPad Prism 9 (GraphPad Software).

Online content

Any methods, additional references, Nature Portfolio reporting summaries, source data, extended data, supplementary information, acknowledgements, peer review information; details of author contributions and competing interests; and statements of data and code availability are available at https://doi.org/10.1038/s41586-023-06269-0.

Reporting summary

Further information on research design is available in the Nature Portfolio Reporting Summary linked to this article.

Data availability

All data are available within the article and the Supplementary Information. Gel source images are shown in Supplementary Fig. 1. Source data are provided with this paper.

1. Jiang, X., Stockwell, B. R. & Conrad, M. Ferroptosis: mechanisms, biology and role in disease. *Nat. Rev. Mol. Cell Biol.* **22**, 266–282 (2021).
2. Mao, C. et al. DHODH-mediated ferroptosis defence is a targetable vulnerability in cancer. *Nature* **593**, 586–590 (2021).
3. Doll, S. et al. FSP1 is a glutathione-independent ferroptosis suppressor. *Nature* **575**, 693–698 (2019).
4. Zhang, L. et al. Recent advances of human dihydroorotate dehydrogenase inhibitors for cancer therapy: current development and future perspectives. *Eur. J. Med. Chem.* **232**, 114176 (2022).
5. Baumgartner, R. et al. Dual binding mode of a novel series of DHODH inhibitors. *J. Med. Chem.* **49**, 1239–1247 (2006).
6. Mishima, E. et al. A non-canonical vitamin K cycle is a potent ferroptosis suppressor. *Nature* **608**, 778–783 (2021).
7. Seiler, A. et al. Glutathione peroxidase 4 senses and translates oxidative stress into 12/15-lipoxygenase dependent- and AIF-mediated cell death. *Cell Metab.* **8**, 237–248 (2008).
8. Wu, J. et al. Intercellular interaction dictates cancer cell ferroptosis via NF2-YAP signalling. *Nature* **572**, 402–406 (2019).
9. Chen, Y. et al. Quantitative profiling of protein carbonylations in ferroptosis by an aniline-derived probe. *J. Am. Chem. Soc.* **140**, 4712–4720 (2018).
10. Moreno, S. G., Laux, G., Brielmeier, M., Bornkamm, G. W. & Conrad, M Testis-specific expression of the nuclear form of phospholipid hydroperoxide glutathione peroxidase (PHGPx). *Biol. Chem.* **384**, 635–643 (2005).
11. Schneider, M. et al. Embryonic expression profile of phospholipid hydroperoxide glutathione peroxidase. *Gene Expr. Patterns* **6**, 489–494 (2006).
12. Liang, H. et al. Short form glutathione peroxidase 4 is the essential isoform required for survival and somatic mitochondrial functions. *J. Biol. Chem.* **284**, 30836–30844 (2009).
13. Conrad, M. et al. The nuclear form of phospholipid hydroperoxide glutathione peroxidase is a protein thiol peroxidase contributing to sperm chromatin stability. *Mol. Cell. Biol.* **25**, 7637–7644 (2005).
14. Schneider, M. et al. Mitochondrial glutathione peroxidase 4 disruption causes male infertility. *FASEB J.* **23**, 3233–3242 (2009).
15. Wu, S. et al. A ferroptosis defense mechanism mediated by glycerol-3-phosphate dehydrogenase 2 in mitochondria. *Proc. Natl Acad. Sci. USA* **119**, e2121987119 (2022).
16. Walse, B. et al. The structures of human dihydroorotate dehydrogenase with and without inhibitor reveal conformational flexibility in the inhibitor and substrate binding sites. *Biochemistry* **47**, 8929–8936 (2008).
17. Christian, S. et al. The novel dihydroorotate dehydrogenase (DHODH) inhibitor BAY 2402234 triggers differentiation and is effective in the treatment of myeloid malignancies. *Leukemia* **33**, 2403–2415 (2019).
18. Varadi, M. et al. AlphaFold Protein Structure Database: massively expanding the structural coverage of protein-sequence space with high-accuracy models. *Nucleic Acids Res.* **50**, D439–D444 (2022).
19. Feng, Y. et al. Structural insight into the type-II mitochondrial NADH dehydrogenases. *Nature* **491**, 478–482 (2012).

Acknowledgements The authors would like to thank A. Wahida for critical reading of the manuscript. This work was supported by funding from the Deutsche Forschungsgemeinschaft (DFG) (CO 291/7-1) and the DFG Priority Program SPP 2306 (CO 291/9-1, 461385412 and CO 291/10-1, 461507177), the German Federal Ministry of Education and Research (BMBF) FERROPath (01EJ2205B), and the European Research Council (ERC) under the European Union's Horizon 2020 research and innovation programme (grant agreement no. GA 884754) to M.C.; JSPS KAKENHI (20KK0363) to E.M.; Alexander von Humboldt Post-Doctoral Fellowship to J.Z.; and China Scholarship Council to W.Z.

Author contributions E.M., T.N., J.Z., and M.C. conceived the study and wrote the manuscript. E.M., T.N., J.Z., and W.Z. performed the experiments and analysis. A.S.D.M. expressed and purified recombinant FSP1 and DHODH. P.S. performed in silico modelling. All authors read and agreed on the content of the paper.

Competing interests M.C. and P.S. hold patents for some of the compounds described herein, and are co-founders and shareholders of ROSCUE Therapeutics.

Additional information

Supplementary information The online version contains supplementary material available at https://doi.org/10.1038/s41586-023-06269-0.

Correspondence and requests for materials should be addressed to Marcus Conrad.

a

Drug	Disease	Clinical trial	NCT number
Brequinar	Acute myeloid leukemia	Phase I/II	NCT03760666
Vidofludimus			
ASLAN003	Acute myeloid leukemia	Phase II	NCT03451084
PTC299	Acute leukemia	Phase I	NCT03761069
BAY-2402234	Leukemia	Phase I	NCT03404726

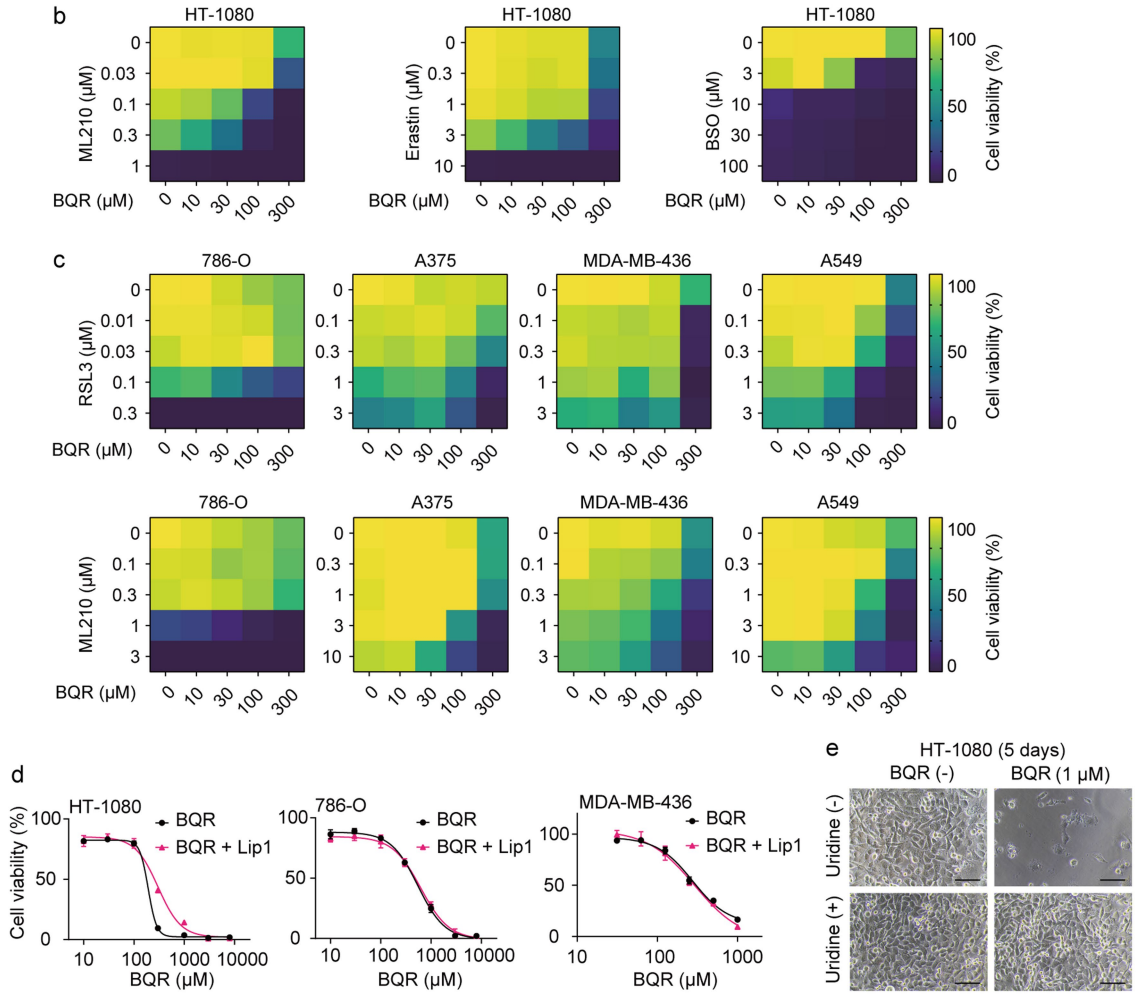

Extended Data Fig. 1 | The synergistic effect of brequinar with ferroptosis inducers in a panel of cancer cell lines. a. Known DHODH inhibitors in cancer-related clinical trials. Sourced from https://clinicaltrials.gov/, August 2022. **b**. Heatmaps of cell viability showing the synergistic effects of brequinar (BQR) with ML210, erastin and BSO in HT-1080 cells. Viability was measured after 48 h (ML210 and erastin) and 72 h treatment (BSO). **c**. Heatmaps of cell viability showing the synergistic effects of BQR with RSL3 and ML210 in 786-O, A375, MDA-MB-436 and A549 cells. Viability was measured after 48 h. **d**. Evaluation of cellular toxicity of brequinar. HT-1080, 786-O and MDA-MB-436 cells were treated with the indicated concentrations of BQR in the presence or absence of the ferroptosis inhibitor liproxstatin-1 (Lip1, 1 μM) for 24 h. BQR treatment alone was not sufficient to induce ferroptosis. **e**. Representative images of HT-1080 cells treated with or without BQR (1 μM) and uridine (100 μM) for 5 days. The cells were seeded at a density of 200 cells/well in a 96-well plate. Scale, 100 μm. Data is mean ± s.d. of n = 3 (d). Data is representative of two independent experiments (b-e).

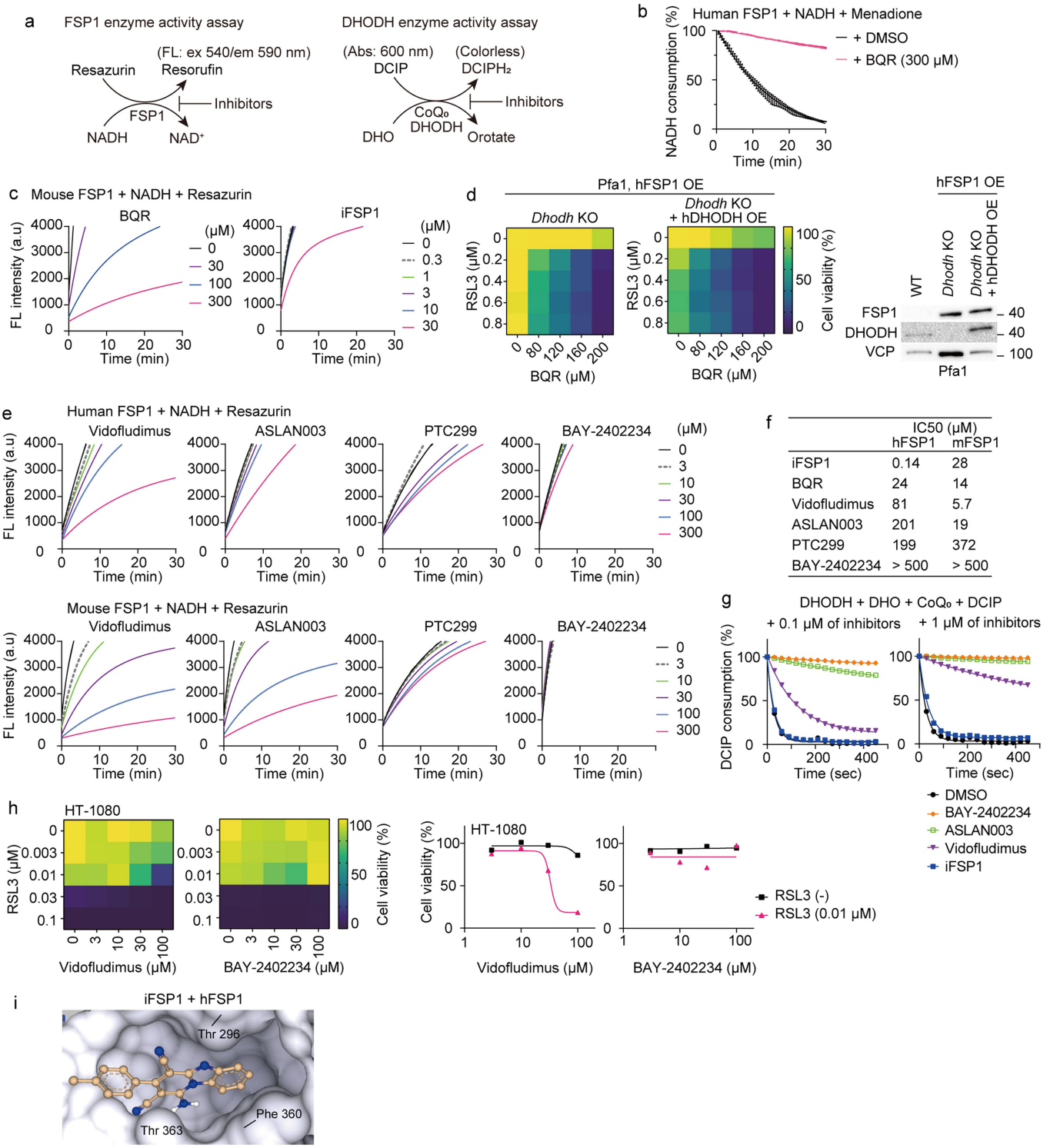

Extended Data Fig. 2 | See next page for caption.

Extended Data Fig. 2 | Inhibitory effects of DHODH inhibitors against FSP1 enzyme activity. a. (Left) Scheme of the FSP1 enzyme activity assay. Resazurin (100 μM), a substrate of FSP1, is reduced to resorufin by incubation with recombinant FSP1 protein (50 and 40 nM of human and mouse FSP1, respectively) and NADH (200 μM). The amount of resorufin evaluated by fluorescent intensity (ex 540/em 590 nm) indicates FSP1 enzymatic activity. (Right) Scheme of the DHODH enzyme activity assay. Enzyme reaction of recombinant human DHODH (25 nM), dihydroorotate (DHO, 500 μM) and CoQ_0 (100 μM) reduces an electron acceptor 2, 6-dichlorophenolindophenol (DCIP, 120 μM) to $DCIPH_2$. The change in absorbance of DCIP (at absorbance 600 nm) indicates DHODH enzyme activity. **b**. NADH consumption assay using recombinant human FSP1 protein (25 nM) in combination with or without brequinar (BQR, 300 μM). Menadione (50 μM) was used as a substrate of FSP1. Brequinar inhibited the FSP1-dependent NADH consumption. **c**. The inhibitory effect of BQR and iFSP1 on mouse FSP1 enzymatic activity. **d**. Heatmaps showing the viability and immunoblotting of hFSP1-overexpressed (OE) and *Dhodh* KO-Pfa1 cells with or without overexpression of hDHODH. Viability was measured after treatment with RSL3 for 24 h. Combination of RSL3 with BQR synergistically induced cell death in both cell lines. **e**. The inhibitory effect of known DHODH inhibitors on human and mouse FSP1 enzyme activity. **f**. Calculated IC_{50} values of iFSP1 and DHODH inhibitors against recombinant human and mouse FSP1. **g**. The inhibitory effect of DHODH inhibitors and iFSP1 against human DHODH enzymatic activity. **h**. Heatmaps showing the viability of HT-1080 cells (5,000 cells per well) treated with RSL3 in combination with vidofludimus or BAY-2402234 for 24 h. The values of the groups treated with zero or 0.01 μM of RSL3 are also shown in the right graphs. **i**. The binding prediction of iFSP1 in human FSP1 protein. Data is mean ± s.d. of n = 3 (b). Data is representative of three (b, c and e) and two independent experiments (d, g and h), respectively.

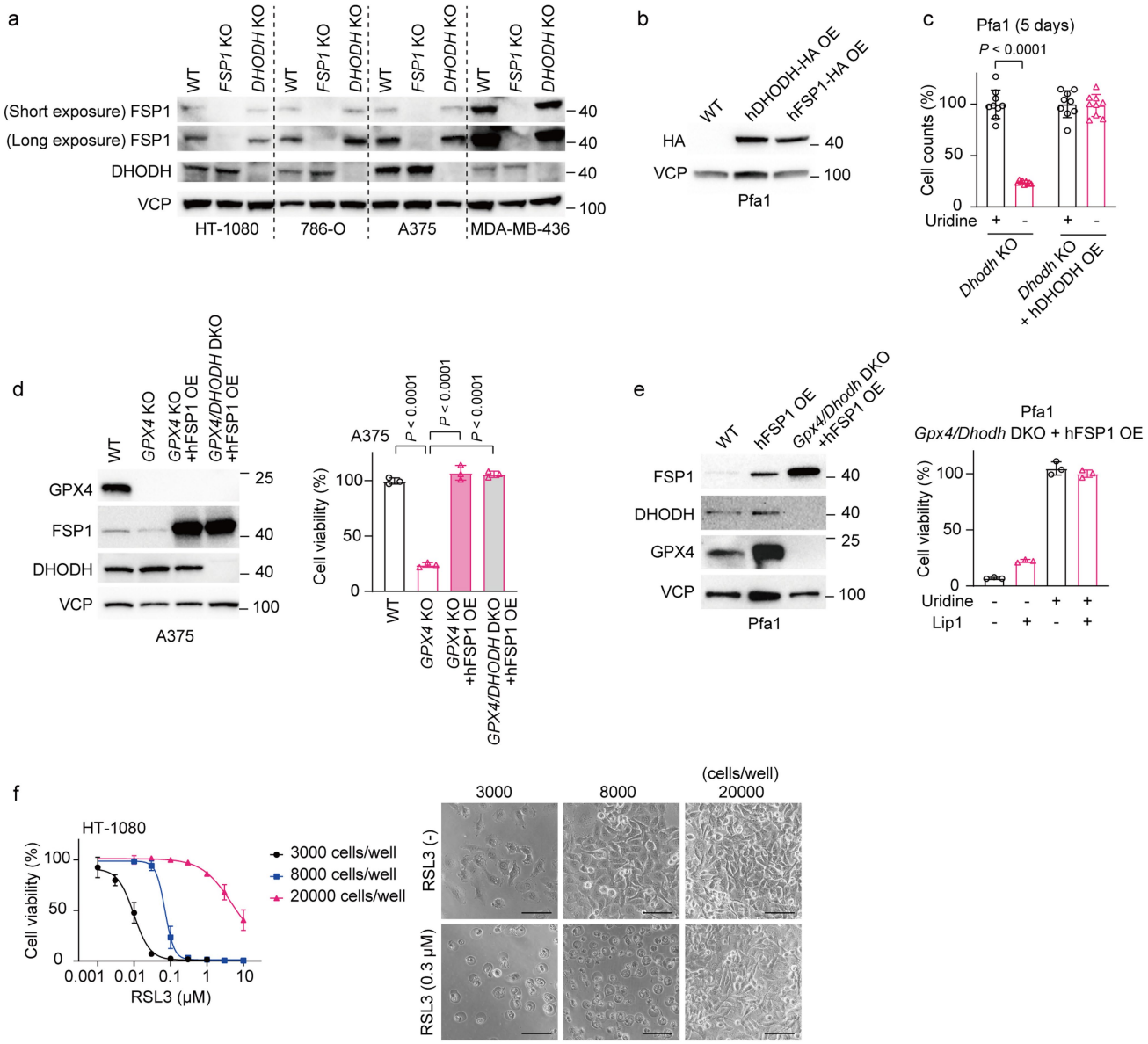

Extended Data Fig. 3 | Immunoblotting of genetic deletion or overexpression of FSP1 and DHODH, and the effect of cell confluency on ferroptosis sensitivity. a. Immunoblotting of lysates of *FSP1* KO and *DHODH* KO cells using HT-1080, 786-O, A375 and MDA-MB-436 cell lines. Each parental cell was used as wild type (WT). **b**. Immunoblotting of lysates of Pfa1 cells with stable overexpression (OE) of C-terminally HA-tagged human DHODH (hDHODH) or FSP1 (hFSP1). One experiment was performed (a, b). **c**. Relative cell counts of *Dhodh* KO Pfa1 cells with or without stable OE of hDHODH seeded 200 cells/well in a 96-well plate and incubated with or without uridine (50 μM) for 5 days. hDHODH OE rescued the suppression of cell growth in *Dhodh* KO Pfa1 cells without uridine supplementation. **d**. Immunoblotting of lysate and viability of A375 cells of WT, *GPX4* KO, *GPX4* KO with hFSP1 OE and *GPX4/DHODH* double KO with hFSP1 OE. For the measurement of the viability, 500 cells/well were seeded in a 96-well plate and incubated with or without Lip1 (1 μM) for 4 days. Viability of the cells incubated with Lip1 (1 μM) was taken as 100%. **e**. Immunoblotting of lysate and viability of *Gpx4* and *Dhodh* double KO Pfa1 cells with stable OE of hFSP1. The cells were seeded at a density of 300 cells/well in a 96-well plate and incubated with or without uridine (50 μM) and Lip1 (1 μM) for 5 days. The *Gpx4* and *Dhodh* double KO Pfa1 cells with OE of hFSP1 cells can survive without Lip1. **f**. The effect of cell density of HT-1080 cells on RSL3-induced cell death. The cells were seeded at densities of 3,000, 8,000 or 20,000 cells/well in a 96-well plate. On the next day, the cells were treated with RSL3 for 6 h and viability was determined. Scale, 100 μm. Data is mean ± s.d. of n = 9 (c) and n = 3 (d-f). Two-tailed *t*-test (c); one-way ANOVA with Dunnett's test (d).

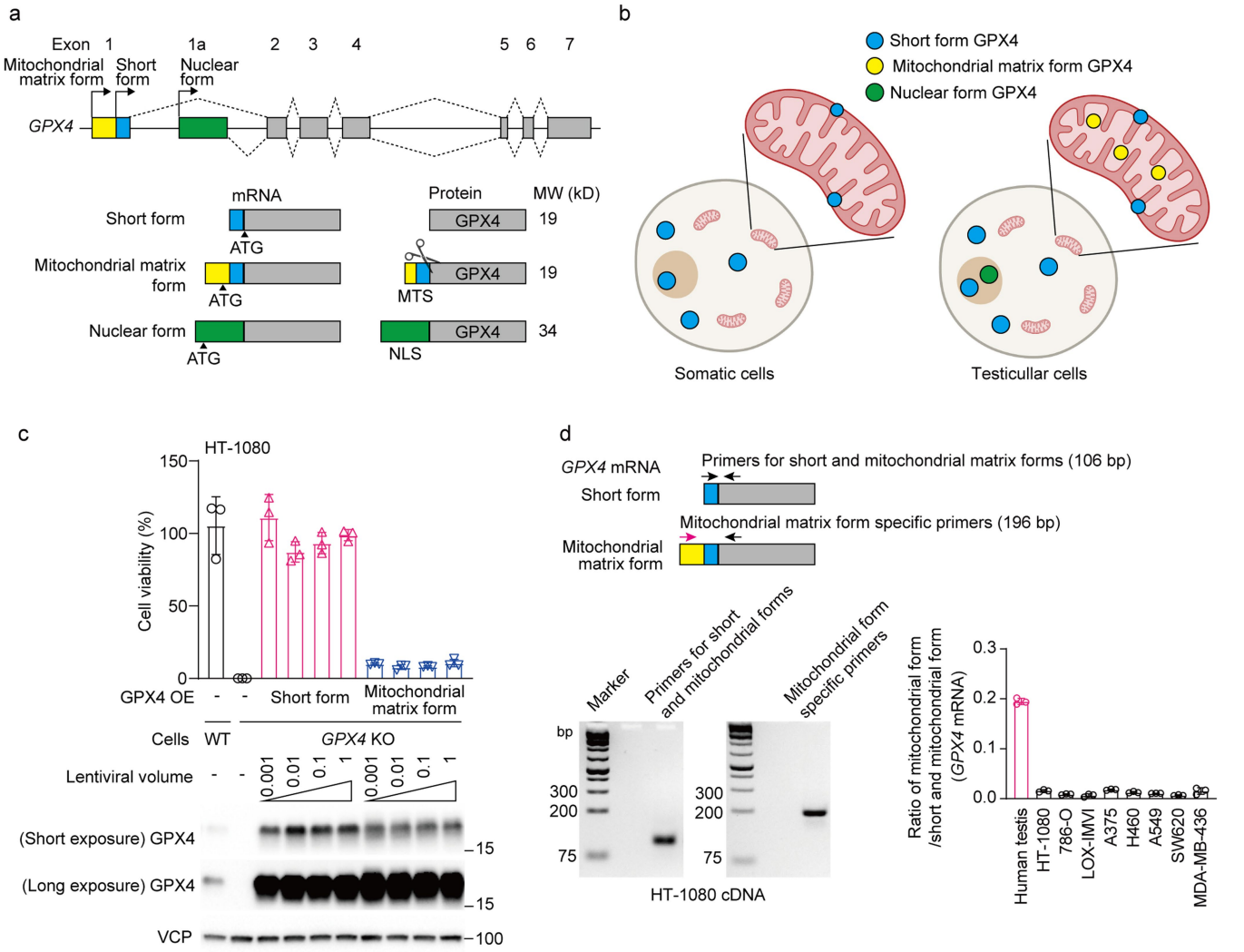

Extended Data Fig. 4 | Expression pattern and subcellular localization of GPX4 isoforms. a. Structural organization of the *GPX4* gene, mRNA and protein of the GPX4 isoforms. Arrows indicate the transcription initiation sites. The dashed lines indicate the different splicing variants. ATG indicates the initiation codon of methionine. MTS, mitochondrial targeting sequence; NLS, nuclear localization signal. NLS also functions for stretching of DNA binding motifs. **b**. A scheme depicting the reported subcellular localization of each GPX4 isoform in somatic and testicular cells. The short form is abundantly expressed in the cytoplasm and mitochondrial extra-matrix space of somatic cells, while the mitochondrial matrix form is abundantly expressed in the mitochondrial matrix of testicular cells. The illustration was created using BioRender.com (a, b). **c**. Viability of *GPX4* KO HT-1080 cells (500 cells/well) overexpressing the short or mitochondrial matrix form of GPX4 for three days after withdrawal of ferrostatin-1 (a ferroptosis inhibitor). The cells were prepared by infection with the indicated serial dilution of lentiviral particles containing the expression plasmids. Immunoblotting validated the overexpression of each form. Viability of the cells incubated with Lip1 (1 μM) was taken as 100%. **d**. The design of the primer pairs detecting both the short and mitochondrial matrix forms (106 bp) and specific for the mitochondrial matrix form (196 bp). Agarose gel images show the amplification of the specific single band. The ratio of the mitochondrial matrix form/short and mitochondrial matrix forms of *GPX4* mRNA expression in the cancer cell lines was calculated as $2^{-\Delta CT}$ in quantitative RT-PCR. Data is representative of two independent experiments (c and d). Data is mean ± s.d. of n = 3 (c and d).

nature portfolio

Corresponding author(s): Marcus Conrad

Last updated by author(s): Feb 23, 2023

Reporting Summary

Nature Portfolio wishes to improve the reproducibility of the work that we publish. This form provides structure for consistency and transparency in reporting. For further information on Nature Portfolio policies, see our Editorial Policies and the Editorial Policy Checklist.

Statistics

For all statistical analyses, confirm that the following items are present in the figure legend, table legend, main text, or Methods section.

n/a	Confirmed	
☐	☒	The exact sample size (*n*) for each experimental group/condition, given as a discrete number and unit of measurement
☐	☒	A statement on whether measurements were taken from distinct samples or whether the same sample was measured repeatedly
☐	☒	The statistical test(s) used AND whether they are one- or two-sided *Only common tests should be described solely by name; describe more complex techniques in the Methods section.*
☒	☐	A description of all covariates tested
☐	☒	A description of any assumptions or corrections, such as tests of normality and adjustment for multiple comparisons
☐	☒	A full description of the statistical parameters including central tendency (e.g. means) or other basic estimates (e.g. regression coefficient) AND variation (e.g. standard deviation) or associated estimates of uncertainty (e.g. confidence intervals)
☐	☒	For null hypothesis testing, the test statistic (e.g. *F*, *t*, *r*) with confidence intervals, effect sizes, degrees of freedom and *P* value noted *Give P values as exact values whenever suitable.*
☒	☐	For Bayesian analysis, information on the choice of priors and Markov chain Monte Carlo settings
☒	☐	For hierarchical and complex designs, identification of the appropriate level for tests and full reporting of outcomes
☒	☐	Estimates of effect sizes (e.g. Cohen's *d*, Pearson's *r*), indicating how they were calculated

Our web collection on statistics for biologists contains articles on many of the points above.

Software and code

Policy information about availability of computer code

Data collection	Image Lab v6.0 (Biorad), SoftMax Pro 7 (Molecular Devices).
Data analysis	GraphPad Prism v9.5 (GraphPad Software), AlphaFold2 database (https://alphafold.ebi.ac.uk), Pymol v2.5.2 (Schrödinger), seeSAR v12.1 (BioSoveIT).

For manuscripts utilizing custom algorithms or software that are central to the research but not yet described in published literature, software must be made available to editors and reviewers. We strongly encourage code deposition in a community repository (e.g. GitHub). See the Nature Portfolio guidelines for submitting code & software for further information.

Data

Policy information about availability of data

All manuscripts must include a data availability statement. This statement should provide the following information, where applicable:

- Accession codes, unique identifiers, or web links for publicly available datasets
- A description of any restrictions on data availability
- For clinical datasets or third party data, please ensure that the statement adheres to our policy

All data are available within the article and the supplementary information. Gel source images are shown in Supplementary figure.

Human research participants

Policy information about studies involving human research participants and Sex and Gender in Research.

Reporting on sex and gender	n.a.
Population characteristics	n.a.
Recruitment	n.a.
Ethics oversight	n.a.

Note that full information on the approval of the study protocol must also be provided in the manuscript.

Field-specific reporting

Please select the one below that is the best fit for your research. If you are not sure, read the appropriate sections before making your selection.

☒ Life sciences ☐ Behavioural & social sciences ☐ Ecological, evolutionary & environmental sciences

For a reference copy of the document with all sections, see nature.com/documents/nr-reporting-summary-flat.pdf

Life sciences study design

All studies must disclose on these points even when the disclosure is negative.

Sample size	Sample sizes in vitro experiments were determined based on the numbers required to achieve statistical significance using indicated statistics, as well as considering of previous publications on similar experiments (PMID: 31634899 and 35922516).
Data exclusions	No data exclusions.
Replication	The experimental findings were reproduced as validated by at least two independent experiment in Fig1 and Extended fig 1-4.
Randomization	Randomization is not relevant to the in vitro experiments since cells come in millions of populations and are automatically randomized and seeded to different wells for treatment.
Blinding	In the in vitro experiments, the investigators were not blinded, which is standard in this type of study due to the multiple steps involved that require precise operations for accuracy and precision precluding blinding to experimental variables.

Reporting for specific materials, systems and methods

We require information from authors about some types of materials, experimental systems and methods used in many studies. Here, indicate whether each material, system or method listed is relevant to your study. If you are not sure if a list item applies to your research, read the appropriate section before selecting a response.

Materials & experimental systems

n/a	Involved in the study
☐	☒ Antibodies
☐	☒ Eukaryotic cell lines
☒	☐ Palaeontology and archaeology
☒	☐ Animals and other organisms
☒	☐ Clinical data
☒	☐ Dual use research of concern

Methods

n/a	Involved in the study
☒	☐ ChIP-seq
☒	☐ Flow cytometry
☒	☐ MRI-based neuroimaging

Antibodies

Antibodies used	GPX4 (1:1000 for WB, ab125066, Abcam), FSP1 (1:1000 for WB, sc-377120, Santa Cruz Biotechnology), DHODH (1:1000 for WB, sc-166348, Santa Cruz Biotechnology), HA antibody (1:1000 for WB, clone 3F10, rat IgG1, developed in-house), valosin containing protein (VCP, 1:10000 for a loading control in WB analysis, ab109240, Abcam).
Validation	GPX4 antibody (ab125066, Abcam) and human FSP1 antibody (sc-377120, Santa Cruz Biotechnology) were validated for WB in

Validation	previous publications (PMID: 31634899 and 35922516). HA antibody was validated for WB in a previous publication (PMID: 31634899). VCP antibody (ab109243, Abcam) was validated for WB on the manufacturer's website (https://www.abcam.com/vcp-antibody-epr33072-ab109240.html). DHODH antibody (c-166348, Santa Cruz Biotechnology) was validated for WB on the manufacturer's website (https://www.scbt.com/p/dhodh-antibody-e-8).

Eukaryotic cell lines

Policy information about cell lines and Sex and Gender in Research

Cell line source(s)	4-OH-TAM-inducible Gpx4-/- murine immortalized fibroblasts (Pfa1) were originally established in our lab and were reported previously (PMID: 18762024). HT-1080 (CCL-121), 786-O (CRL-1932), A375 (CRL-1619), MDA-MB-436 (HTB-130), A549 (CCL-185), H460 (HTB-177), SW620 (CCL-227) and HEK293T (CRL-3216) cells were obtained from ATCC. LOX-IMVI was obtained from NCI/NIH.
Authentication	None of the cell lines used were authenticated.
Mycoplasma contamination	All cell lines were tested negative for mycoplasma contamination.
Commonly misidentified lines (See ICLAC register)	No commonly misidentified cell lines were used.

Reply to: DHODH inhibitors sensitize to ferroptosis by FSP1 inhibition

https://doi.org/10.1038/s41586-023-06270-7

Published online: 5 July 2023

Check for updates

Chao Mao[1], Xiaoguang Liu[1], Yuelong Yan[1], Kellen Olszewski[2] & Boyi Gan[1]✉

REPLYING TO E. Mishima et al. *Nature* https://doi.org/10.1038/s41586-023-06269-0 (2023)

Ferroptosis represents a form of cell death induced by excessive lipid peroxidation on cellular membranes[1,2]. Our recent study identified a defence mechanism in mitochondria mediated by dihydroorotate dehydrogenase (DHODH) via ubiquinol generation[3]. In the accompanying Comment[4], Mishima et al. were able to reproduce our findings that *DHODH* deletion or treatment with the DHODH inhibitor brequinar sensitized cancer cells to ferroptosis. However, they argue that: (1) ferroptosis-sensitization phenotypes in *DHODH*-knockout cells are mild—therefore, DHODH has a limited role in ferroptosis regulation; (2) ferroptosis sensitization by brequinar (and other DHODH inhibitors) is mediated by their off-target effects through inhibition of ferroptosis suppressor protein 1 (FSP1), another critical mediator of ferroptosis defence[5,6]; and (3) our data revealing a role of mitochondrial GPX4 in regulating ferroptosis is inconsistent with the current understanding of different GPX4 isoforms. Below we provide our counter-argument and clarification.

Mishima et al.[4] criticized our study for using high concentrations of RSL3 and high cell densities to study ferroptosis. The study was designed to identify potential ferroptosis defence mechanisms that presumably are turned on following acute GPX4 inactivation (by two-hour treatment with RSL3; figure 1a in ref. 3). Correspondingly, we have focused mainly on studying ferroptosis in response to short-term (four-hour) treatment with RSL3 in subsequent analyses. In addition, long-term treatment with DHODH inhibitors induces strong cell cycle arrest, which would complicate the interpretation of the results from cell viability measurements. For these reasons, we used high doses of RSL3 with high cell densities in our analyses so that ferroptosis can be induced within a short time frame. Notably, we confirm that treatment with the ferroptosis inhibitors ferrostatin-1 or liproxstatin-1, or genetic ablation of *ACSL4* largely restored the decreased cell viability caused by RSL3 treatment (Fig. 1a; also see figure 1j and extended data figure 3i in ref. 3); therefore, regardless of the effect of cell density on ferroptosis sensitivity, the cell death induced under our experimental conditions was indeed ferroptosis. We also observed that, when seeded at the same cell numbers, the densities of HT-1080 cells from our experiments were much lower than those shown in extended data figure 3f by Mishima et al.[4], probably reflecting differences in cell growth conditions or experimental design between different laboratories. Notably, we confirm that *DHODH* deletion promoted ferroptosis induced by *GPX4* ablation in HT-1080 and 786-O cells (Fig. 1b,c and Extended Data Fig. 1a), and also showed that *DHODH* deletion in GPX4^{low} NCI-H226 and HCT 116 cells was sufficient to trigger ferroptosis (Fig. 1d and Extended Data Fig. 1b; also see figure 2e in ref. 3); these results would be independent of the potential confounding effects caused by differences in RSL3 dose or treatment duration, because RSL3 was not used in these experiments. Therefore, our genetic data establishing a role of DHODH in ferroptosis protection are solid.

In our recent study, we proposed a compartmentalization model in ferroptosis defence[3], wherein cytosolic GPX4 and FSP1 operates as a separate defence system to mitochondrial GPX4 and DHODH, the two systems together quenching non-mitochondrial and mitochondrial lipid peroxides, respectively. This leads to two different scenarios in ferroptosis-inducing conditions, depending on the status of DHODH: (1) in wild-type *DHODH* cells, GPX4 inactivation triggers ferroptosis primarily through inducing non-mitochondrial lipid peroxidation (under which condition DHODH keeps mitochondria in check under GPX4 inactivation); and (2) DHODH inactivation significantly weakens the defence system in mitochondria; consequently, in DHODH and GPX4 double-inactive cells, ferroptosis is primarily induced by mitochondrial lipid peroxidation. Space limits prevented us from discussing this model in detail in our publication, which might have contributed to a misunderstanding of our model by Mishima et al.[4]—we subsequently published a perspective that discussed this model extensively[7]. For example, they argued that our data showing that mitochondrial GPX4 had more protective effects than cytosolic GPX4 in *GPX4*-knockdown cells treated with brequinar (see figure 3b and extended data figure 5g in ref. 3) contradicted our subsequent observation that cytosolic GPX4, but not mitochondrial GPX4, rescued ferroptosis in *GPX4*-knockout cells (see figure 4k in ref. 8). However, these two observations were derived from very different contexts. Specifically, because ferroptosis is induced mainly by non-mitochondrial lipid peroxidation in *GPX4*-knockout cells, cytosolic GPX4 (but not mitochondrial GPX4) suppressed ferroptosis induced by *GPX4* deletion (with intact DHODH). By contrast, because ferroptosis is induced mainly by mitochondrial lipid peroxidation in brequinar-treated *GPX4*-knockdown cells (with inactive DHODH), the protective effect by GPX4 shifted such that mitochondrial GPX4 had more protective effect than cytosolic GPX4 in this context. Furthermore, based on our model, it is indeed expected that DHODH overexpression would have a limited effect on suppressing ferroptosis in *GPX4*-knockout cells (shown by Mishima et al.[4] in their figure 1i, as one line of evidence arguing against a role of DHODH in ferroptosis regulation), because increasing mitochondrial ubiquinol production and strengthening ferroptosis defence in mitochondria would not significantly alleviate ferroptosis primarily triggered by non-mitochondrial lipid peroxidation in *GPX4*-knockout cells.

Mishima et al.[4] also showed that brequinar treatment sensitized wild-type cells, but not *FSP1*-knockout counterparts, to RSL3-induced ferroptosis, enabling them to conclude that brequinar treatment promotes ferroptosis through inactivating FSP1. However, this observation can also be explained by the compartmentalization model. Inactivation of cytosolic GPX4 and FSP1 rendered cells extremely vulnerable to ferroptosis induced by non-mitochondrial lipid peroxidation, under which condition further weakening ferroptosis defence in mitochondria

[1]Department of Experimental Radiation Oncology, The University of Texas MD Anderson Cancer Center, Houston, TX, USA. [2]The Barer Institute, Philadelphia, PA, USA.
✉e-mail: bgan@mdanderson.org

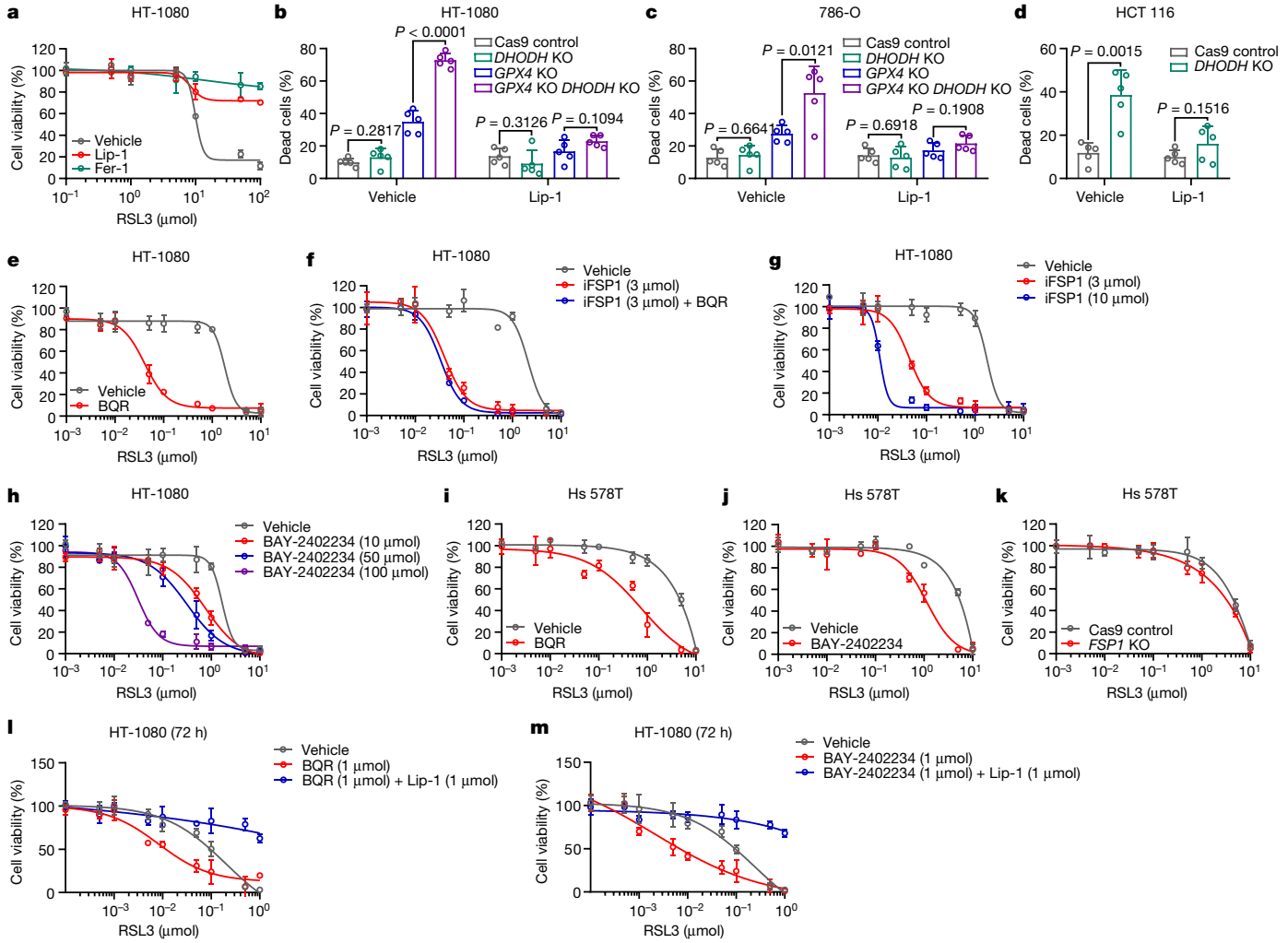

Fig. 1 | Analyses of ferroptosis phenotypes in cells with DHODH deletion or DHODH inhibitor treatment. a, Cell viability measurements in HT-1080 cells treated with RSL3, liproxstatin-1 (Lip-1; 10 μM) and/or ferrostatin-1 (Fer-1; 10 μM) for 4 h. **b**, Cell death measurements in HT-1080 cells with indicated genotypes treated with vehicle and Lip-1 (0.1 μM) for 3 days. **c**, Cell death measurements in 786-O cells with indicated genotypes treated with vehicle and Lip-1 (0.1 μM) for 4 days. **d**, Cell death measurements in Cas9 control and *DHODH*-knockout (KO) HCT 116 cells treated with vehicle and Lip-1 (0.1 μM) for 6 days. **e**, Cell viability measurements in HT-1080 cells treated with RSL3 and brequinar (BQR; 100 μM) for 24 h. **f**, Cell viability measurements in HT-1080 cells treated with RSL3, FSP1-specific inhibitor iFSP1 (3 μM) and brequinar (100 μM) for 24 h. **g**, Cell viability measurements in HT-1080 cells treated with RSL3 and iFSP1 (3 μM or 10 μM) for 24 h. **h**, Cell viability measurements in HT-1080 cells treated with RSL3 and BAY-2402234 (10 μM, 50 μM or 100 μM) for 24 h. **i**, Cell viability measurements in Hs 578T cells treated with RSL3 and brequinar (100 μM) for 24 h. **j**, Cell viability in Hs 578T cells treated with RSL3 and BAY-2402234 (100 μM) for 24 h. **k**, Cell viability measurements in Cas9 control and *FSP1*-knockout Hs 578T cells treated with RSL3 for 24 h. **l**, Cell viability measurements in HT-1080 cells treated with RSL3, brequinar (1 μM) and Lip-1 (1 μM) for 72 h. **m**, Cell viability measurements in HT-1080 cells treated with RSL3, BAY-2402234 (1 μM) and Lip-1 (1 μM) for 72 h. **b**–**m**, Cells were grown in medium supplemented with 50 μM uridine. Data are mean ± s.d. of $n = 3$ (**a**,**e**–**m**) or $n = 5$ (**b**–**d**). Data are from at least three independent replicates. Statistical analysis was performed using unpaired, two-tailed *t*-test.

(by DHODH inactivation) does not further promote ferroptosis. In line with this, we showed that brequinar sensitized HT-1080 cells to RSL3 but did not increase RSL3 sensitization under iFSP1 treatment (Fig. 1e,f). Our rationale was that, if brequinar promoted ferroptosis through inactivating FSP1, the combination of two FSP1 inhibitors (brequinar and iFSP1) would be expected to further enhance RSL3 sensitivity. Of note, further enhancing iFSP1 concentrations increased RSL3 sensitization; therefore, the lack of ferroptosis-sensitization effect by brequinar in cells treated with 3 μM iFSP1 was not caused by a complete inactivation of FSP1 under this condition (Fig. 1g). Another key piece of evidence allowing us to separate DHODH from FSP1 in regulating ferroptosis is the different phenotypes in DHODH-inactive cells compared with FSP1-inactive cells in induction of mitochondrial lipid peroxidation: DHODH inactivation (genetically or pharmacologically), but not FSP1 inactivation, induced potent mitochondrial lipid peroxidation when combined with GPX4 inactivation (see figure 3f and extended data figure 6f–n in ref. 3).

Notably, the DHODH inhibitors that we tested—regardless of their structural similarity to iFSP1 (Extended Data Fig. 1c–i) or their ability to inhibit FSP1—strongly sensitized HT-1080 cells to RSL3 (Fig. 1e,h and Extended Data Fig. 1j–m). In particular, although they showed that BAY-2402234 did not affect RSL3 sensitivity at 100 μM and did not inhibit FSP1 activity at 300 μM, we found that BAY-2402234 significantly sensitized HT-1080 cells to RSL3 at 100 μM or lower concentrations (Fig. 1h). Furthermore, DHODH inhibitor treatment increased RSL3 sensitivity in Hs 578T cells, whereas *FSP1* deletion or overexpression did not affect RSL3 sensitivity in this cell line (Fig. 1i–k and Extended Data Fig. 1n–p). We also tested the effect of DHODH inhibitors on ferroptosis at a dose that could completely suppress cell proliferation. Mishima et al.[4] showed in figure 1b that brequinar completely suppressed cell proliferation in

HT-1080 cells at 1 μM (which is substantially lower than the concentration required to inhibit FSP1) over 5 days (without uridine supplementation and with a very low cell seeding). Using similar cell seeding conditions, we found that brequinar or BAY-2402234 treatment at 1 μM sensitized HT-1080 cells to RSL3-induced ferroptosis over 1- or 3-day treatments (with uridine supplementation; Fig. 1l,m and Extended Data Fig. 1q,r). Together, our data argue against the conclusion that DHDOH inhibitors promote ferroptosis through FSP1 under all conditions.

Finally, it was argued that mitochondrial GPX4 (or the mitochondrial matrix form of GPX4, as described by Mishima et al.[4]) was expressed at much lower levels than cytosolic GPX4 (or short-form GPX4). Our analyses by fractionation confirmed that there are lower levels of GPX4 protein in the mitochondrial fraction than in the cytosolic fraction; nevertheless, GPX4 can clearly be detected in mitochondrial fraction (see extended data figure 5a in ref. 3). It can be argued that substantial GPX4 detected in mitochondrial fraction might represent cytosolic, short-form GPX4 translocated into mitochondria, because it was previously reported that cytosolic, short-form GPX4 was significantly enriched in the intermembrane space of mitochondria[9]. However, our data showed that cytosolic, short-form GPX4 localizes mainly in the cytosol without an appreciable detection in mitochondria (see extended data figure 5c in ref. 3 and figure 4g in ref. 8). This discrepancy is likely to result from the different methods used to study GPX4 localization in these studies: in our studies[3,8], we re-expressed cytosolic or mitochondrial GPX4 in *GPX4*-knockout (or knockdown) cells and measured their localization by fractionation[3,8]—whereas in the other study[9], the authors mutated the translation start site ATG in the endogenous locus encoding mitochondrial *GPX4* and studied the resulting animals and cells, which presumably only express cytosolic GPX4. The extent to which and how cytosolic GPX4 can translocate to mitochondria remain to be further studied.

Note added in proof: Several recent studies (including those using genetic approaches) have validated the role of DHODH in suppressing ferroptosis under different contexts[10–13].

Methods

Cell culture studies

Cancer cell lines were obtained from the American Type Culture Collection. All cell lines were free of mycoplasma contamination (tested by the vendor). No cell line used in this study has been found in the International Cell Line Authentication Committee database of commonly misidentified cell lines, based on short tandem repeat profiling performed by the vendor. Parental cells were cultured in EMEM (HT-1080), RPMI-1640 (786-O), DMEM (293T, Hs 578T) or McCoy's 5a (HCT 116) medium with 10% (volume/volume; v/v) FBS and 1% (v/v) penicillin/streptomycin at 37 °C with a humidified atmosphere of 20% O_2 and 5% CO_2.

CRISPR–Cas9-mediated gene knockout

Knockout of *GPX4*, *DHODH* and *FSP1* in human cell lines was performed using CRISPR-V2 vector (Addgene, #52961). In brief, 293T cells were transfected with CRISPR-V2 constructs, together with psPAX.2 and pMD2.G third-generation lentiviral packaging system using Lipofectamine 2000 reagent (Life Technologies) according to the manufacturer's instructions. 72 h later, lentivirus particles in the medium were collected and filtered, then the target cell lines were infected. At 48 h post-infection, 2 μg ml^{-1} puromycin was added to obtain stable cell lines with successful transduction. *GPX4*-knockout cells were selected in Lip-1 (0.1 μM)-supplemented medium. *DHODH*-knockout cells were selected in Lip-1 (0.1 μM) + uridine (50 μM)-supplemented medium. Each cell line was verified by western blot to confirm the target gene deletion. The oligo sequences preceding the protospacer motif were: *GPX4* guide, 5′-caccgGGTGAAGCGCTACGGACCCA-3′; *DHODH* guide, 5′-caccgTGAGTTGATAAATCCCGGAG-3′; *FSP1* guide, 5′-caccgTCCCGATTCCACCGAGACCT-3′.

Overexpression cell line generation

293T cells were transfected with either pLVX-empty vector or FSP1 constructs, together with psPAX.2 and pMD2.G third-generation lentiviral packaging system. Seventy-two hours later, lentivirus particles in the medium were collected and filtered, then the target cell lines were infected. At 48 h after infection, 2 μg ml^{-1} puromycin was added to obtain stable cell lines with successful transduction. Each cell line was verified by western blot to confirm the target gene deletion.

Immunoblotting

Cell pellets and tissues were lysed using IP lysis buffer (Fisher Scientific) and the protein concentration was determined by a Bicinchoninic Acid Protein Assay (Thermo Scientific) using a FLUOstar Omega microplate reader (BMG Labtech). 25 μg of protein was used for immunoblot analysis using antibodies against GPX4 (1:1,000, MAB5457, R&D Systems), DHODH (1:1,000, 14877-1-AP, Proteintech), FSP1 (1:1,000, sc-377120, Santa Cruz Biotechnology) and vinculin (1:3,000, V4505, Sigma-Aldrich).

Cell viability and death assay

Viable cells were measured using Cell Counting Kit-8 (CCK-8, Dojindo). For the experiment described in Fig. 1a, HT-1080 cells were seeded onto 96-well plates at a density of 2×10^4 per well. For the experiment described in Fig. 1l,m and Extended Data Fig. 1q,r, HT-1080 cells were seeded onto 96-well plates at a density of 0.4×10^3 per well. For other experiments, cells were seeded onto 96-well plates at a density of 8×10^3 (HT-1080) or 6×10^3 (Hs 578T) per well. On the next day, cells were treated with GPX4, FSP1 or DHODH inhibitors with indicated doses and treatment duration as described in figure legends. Subsequently, cells were exposed to 20 μl CCK-8 reagent (200 μl medium per well) for 1 h at 37 °C, 5% CO_2 in an incubator. The absorbance at a wavelength of 450 nm was determined using a Synergy 2 microplate reader (BioTek) and data connected by BioTek Gen5. Cell death was measured using trypan blue staining. In brief, cells were seeded onto 10-cm tissue culture dishes at a density of 4×10^5 per dish and passaged at 1:3 every 3 (HT-1080) or 4 (786-O and HCT 116) days. Cells were suspended and stained with 0.4% trypan blue solution (Thermo Fisher Scientific). Dead cells were blue and live cells were transparent. Dead cells (%) were calculated by using the following formula: 100 × (no. of dead cells)/(no. of dead cells + no. of live cells).

Statistics and reproducibility

Results of cell culture experiments were collected from at least three independent replicates. Data are presented as mean ± s.d. Statistical significance (*P* values) was calculated using unpaired Student's *t*-tests in GraphPad Prism 8.0.1.

Online content

Any methods, additional references, Nature Portfolio reporting summaries, source data, extended data, supplementary information, acknowledgements, peer review information; details of author contributions and competing interests; and statements of data and code availability are available at https://doi.org/10.1038/s41586-023-06270-7.

Reporting summary

Further information on research design is available in the Nature Portfolio Reporting Summary linked to this article.

Data availability

All data that support the conclusions in this manuscript are available from the corresponding author upon reasonable request.

1. Dixon, S. J. et al. Ferroptosis: an iron-dependent form of nonapoptotic cell death. *Cell* **149**, 1060–1072 (2012).
2. Stockwell, B. R. Ferroptosis turns 10: emerging mechanisms, physiological functions, and therapeutic applications. *Cell* **185**, 2401–2421 (2022).
3. Mao, C. et al. DHODH-mediated ferroptosis defence is a targetable vulnerability in cancer. *Nature* **593**, 586–590 (2021).
4. Mishima, E. et al. DHODH inhibitors sensitize to ferroptosis by FSP1 inhibition. *Nature* https://doi.org/10.1038/s41586-023-06269-0 (2023).
5. Bersuker, K. et al. The CoQ oxidoreductase FSP1 acts parallel to GPX4 to inhibit ferroptosis. *Nature* **575**, 688–692 (2019).
6. Doll, S. et al. FSP1 is a glutathione-independent ferroptosis suppressor. *Nature* **575**, 693–698 (2019).
7. Gan, B. Mitochondrial regulation of ferroptosis. *J. Cell Biol.* **220**, e202105043 (2021).
8. Wu, S. et al. A ferroptosis defense mechanism mediated by glycerol-3-phosphate dehydrogenase 2 in mitochondria. *Proc. Natl Acad. Sci. USA* **119**, e2121987119 (2022).
9. Liang, H. et al. Short form glutathione peroxidase 4 is the essential isoform required for survival and somatic mitochondrial functions. *J. Biol. Chem.* **284**, 30836–30844 (2009).
10. Chen, S. et al. Synergistic functional nanomedicine enhances ferroptosis therapy for breast tumors by a blocking defensive redox system. *ACS Appl. Mater. Interfaces* **15**, 2705–2713 (2023).
11. Li, D. et al. Dihydroorotate dehydrogenase regulates ferroptosis in neurons after spinal cord injury via the P53-ALOX15 signaling pathway. *CNS Neurosci. Ther.* https://doi.org/10.1111/cns.14150 (2023).
12. Yang, C. et al. De novo pyrimidine biosynthetic complexes support cancer cell proliferation and ferroptosis defence. *Nat. Cell Biol.***25**, 836–847 (2023).
13. Zhan, M. et al. Lysyl oxidase-like 3 restrains mitochondrial ferroptosis to promote liver cancer chemoresistance by stabilizing dihydroorotate dehydrogenase. *Nat. Comm.* **14**, 3123 (2023).

Acknowledgements This research was supported by internal fund from the University of Texas MD Anderson Cancer Center.

Author contributions C.M. performed most of the experiments with assistance from X.L. and Y.Y. B.G., C.M. and K.O. designed the experiments. B.G. supervised the study, established collaborations, allocated funding for this study, and wrote most of the manuscript with the assistance from K.O. and C.M. All authors commented on the manuscript. We note that the author list for this Reply differs from the original paper in number and order to accurately reflect its more focused scope compared with the original work.

Competing interests The authors declare no competing interests.

Additional information

Supplementary information The online version contains supplementary material available at https://doi.org/10.1038/s41586-023-06270-7.

Correspondence and requests for materials should be addressed to Boyi Gan.

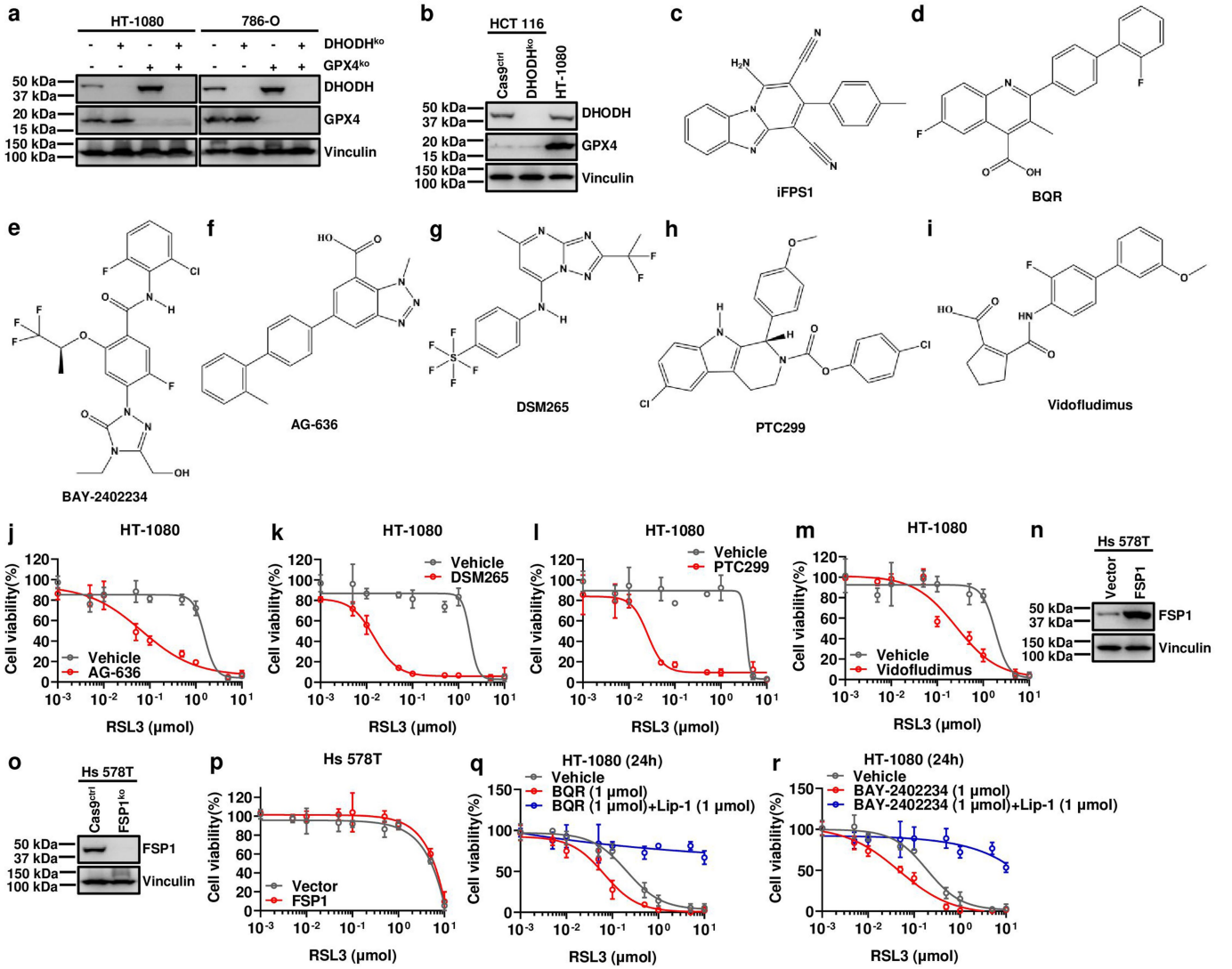

Extended Data Fig. 1 | Analyses of ferroptosis phenotypes in cells with DHODH deletion or DHODH inhibitor treatment. a,**b**, DHODH, GPX4 and Vinculin protein levels in different cell lines were determined by western blotting. **c**–**i**, Chemical structures of iFSP1 (**c**), BQR (**d**), BAY-2402234 (**e**), AG-636 (**f**), DSM265 (**g**), PTC299 (**h**) and Vidofludimus (**i**). **j**–**m**, Cell viability measurement in HT-1080 cells treated with RSL3, AG-636 (100 μM) (**j**), DSM265 (100 μM) (**k**), PTC299 (100 μM) (**l**) and Vidofludimus (100 μM) (**m**) for 24 h. **n**,**o**, FSP1 and Vinculin protein levels in different cell lines were determined by western blotting. **p**, Cell viability measurement in Vector and FSP1 overexpression Hs 578T cells treated with RSL3 for 24 h. **q**, Cell viability measurement in HT-1080 cells treated with RSL3, BQR (1 μM) and Lip-1 (1 μM) for 24 h. **r**, Cell viability measurement in HT-1080 cells treated with RSL3, BAY-2402234 (1 μM) and Lip-1 (1 μM) for 24 h. In **a**,**b**,**j**–**r**, cells were grown in uridine (50 μM) supplemented medium. Data are presented as mean values +/− SD, n = 3 (**j**–**m**,**p**–**r**). Data are from three independent replicates (**j**–**m**,**p**–**r**). Western blot is representative of two independent replicates (**a**,**b**,**n**,**o**).

nature portfolio

Corresponding author(s): Boyi Gan

Last updated by author(s): Mar 9, 2023

Reporting Summary

Nature Portfolio wishes to improve the reproducibility of the work that we publish. This form provides structure for consistency and transparency in reporting. For further information on Nature Portfolio policies, see our Editorial Policies and the Editorial Policy Checklist.

Statistics

For all statistical analyses, confirm that the following items are present in the figure legend, table legend, main text, or Methods section.

n/a	Confirmed	
☐	☒	The exact sample size (*n*) for each experimental group/condition, given as a discrete number and unit of measurement
☐	☒	A statement on whether measurements were taken from distinct samples or whether the same sample was measured repeatedly
☐	☒	The statistical test(s) used AND whether they are one- or two-sided *Only common tests should be described solely by name; describe more complex techniques in the Methods section.*
☒	☐	A description of all covariates tested
☒	☐	A description of any assumptions or corrections, such as tests of normality and adjustment for multiple comparisons
☐	☒	A full description of the statistical parameters including central tendency (e.g. means) or other basic estimates (e.g. regression coefficient) AND variation (e.g. standard deviation) or associated estimates of uncertainty (e.g. confidence intervals)
☐	☒	For null hypothesis testing, the test statistic (e.g. *F*, *t*, *r*) with confidence intervals, effect sizes, degrees of freedom and *P* value noted *Give P values as exact values whenever suitable.*
☒	☐	For Bayesian analysis, information on the choice of priors and Markov chain Monte Carlo settings
☒	☐	For hierarchical and complex designs, identification of the appropriate level for tests and full reporting of outcomes
☒	☐	Estimates of effect sizes (e.g. Cohen's *d*, Pearson's *r*), indicating how they were calculated

Our web collection on statistics for biologists contains articles on many of the points above.

Software and code

Policy information about availability of computer code

Data collection	- BioTek Gen5
Data analysis	- GraphPad Prism version 8.0.1

For manuscripts utilizing custom algorithms or software that are central to the research but not yet described in published literature, software must be made available to editors and reviewers. We strongly encourage code deposition in a community repository (e.g. GitHub). See the Nature Portfolio guidelines for submitting code & software for further information.

Data

Policy information about availability of data

All manuscripts must include a data availability statement. This statement should provide the following information, where applicable:

- Accession codes, unique identifiers, or web links for publicly available datasets
- A description of any restrictions on data availability
- For clinical datasets or third party data, please ensure that the statement adheres to our policy

All data that support the conclusions in this manuscript are available from the corresponding author upon reasonable request.

Human research participants

Policy information about studies involving human research participants and Sex and Gender in Research.

Reporting on sex and gender	N/A
Population characteristics	N/A
Recruitment	N/A
Ethics oversight	N/A

Note that full information on the approval of the study protocol must also be provided in the manuscript.

Field-specific reporting

Please select the one below that is the best fit for your research. If you are not sure, read the appropriate sections before making your selection.

☒ Life sciences ☐ Behavioural & social sciences ☐ Ecological, evolutionary & environmental sciences

For a reference copy of the document with all sections, see nature.com/documents/nr-reporting-summary-flat.pdf

Life sciences study design

All studies must disclose on these points even when the disclosure is negative.

Sample size	No statistical methods were used to pre-determine sample sizes. The number of samples was estimated based on standard practices in the field or pilot studies in our lab.
Data exclusions	Data were not excluded in this study.
Replication	All attempts at replication were successful. The exact number of independent replicates for each experimental group is listed in the corresponding figure legends.
Randomization	We did not carry out any randomization because this is either irrelevant or not applicable to this study.
Blinding	For cell-based experiments and western blotting, cell types were known when prepare the samples or start to treat cells at the beginning of experiments. Investigators were not blinded during experiments and outcome assessments. There were defined groups and blinding was not necessary.

Reporting for specific materials, systems and methods

We require information from authors about some types of materials, experimental systems and methods used in many studies. Here, indicate whether each material, system or method listed is relevant to your study. If you are not sure if a list item applies to your research, read the appropriate section before selecting a response.

Materials & experimental systems

n/a	Involved in the study
☐	☒ Antibodies
☐	☒ Eukaryotic cell lines
☒	☐ Palaeontology and archaeology
☒	☐ Animals and other organisms
☒	☐ Clinical data
☒	☐ Dual use research of concern

Methods

n/a	Involved in the study
☒	☐ ChIP-seq
☒	☐ Flow cytometry
☒	☐ MRI-based neuroimaging

Antibodies

Antibodies used	GPX4 (1:1,000, MAB5457, R&D systems), DHODH (1:1,000, 14877-1-AP, Proteintech), FSP1 (1:1,000, sc-377120, Santa Cruz Biotechnology) and Vinculin (1:3,000, V4505, Sigma-Aldrich). All antibodies were diluted n TBST buffer containing 3% BSA.
Validation	All antibodies used in our study have been validated and detailed information could be found on the website from manufactures as

Validation	listed below. Some of them have also been validated by our experiments as shown in this manuscript using either over-express, knockout or knockdown strategies. DHODH: https://www.ptglab.com/products/DHODH-Antibody-14877-1-AP. GPX4: https://www.rndsystems.com/products/human-mouse-rat-glutathione-peroxidase-4-gpx4-antibody-565320_mab5457. Vinculin: https://www.sigmaaldrich.com/catalog/product/sigma/v4505?lang=en&region=US. FSP1: https://www.scbt.com/p/amid-antibody-b-6.

Eukaryotic cell lines

Policy information about cell lines and Sex and Gender in Research

Cell line source(s)	HT-1080, 786-O, 293T, Hs 578T and HCT 116 cell lines were obtained from the American Type Culture Collection.
Authentication	Cell line were not authenticated.
Mycoplasma contamination	All cell lines tested negative for mycoplasma contamination.
Commonly misidentified lines (See ICLAC register)	No ICLAC cell line was used in this study.